ELSEVIER

Journal of Organometallic Chemistry 637–639 (2001) 304–310

Journal of Organometallic Chemistry

www.elsevier.com/locate/jorganchem

The effect of d-block metal complexation on the spectroscopic and redox properties of ferrocene derivatives containing pyridine ligands

Jonathan D. Carr [a], Simon J. Coles [b], M.B. Hursthouse [b], James H.R. Tucker [a,*]

[a] *School of Chemistry, University of Exeter, Stocker Road, Exeter EX4 4QD, UK*
[b] *Department of Chemistry, University of Southampton, Highfield, Southampton SO17 1BJ, UK*

Received 3 January 2001; received in revised form 16 March 2001; accepted 20 March 2001

Abstract

Three ferrocene derivatives **1**–**3**, each containing two pyridine ligands, form complexes with a variety of d-block metals, as evidenced by NMR and UV–vis spectroscopy and cyclic voltammetry. The X-ray crystal structures of **1** and its Mo(0) complex are reported. The Zn(II) and Cu(I) complexes of **1**–**3** have a 2/1 (ligand/metal) stoichiometry. The factors influencing the changes in the redox and chromogenic properties of these ligands upon complexation are discussed.

Keywords: Ferrocene; Complexes; Sensor; Cyclic voltammetry; Spectroscopy

1. Introduction

There have been numerous accounts over the past two decades of the attachment of ligand groups to ferrocene in order to assess the effect that the ferrocene has on the properties of the proximate binding site and likewise the effect that the binding site has on the properties of the ferrocene. Accordingly, ligands for transition metals [1], s-block cations [2], protons [3], p-block anions [4] and organic molecules, be they charged [5] or neutral [6], have been connected to ferrocene through covalent bonds.

The ferrocene unit can affect the properties of the binding site in a number of ways. For example, redox-switched processes have been demonstrated where oxidation of the ferrocene either decreases [2c] or increases [6] the ligand binding affinity for a substrate. Ferrocenes are also known to quench metal-centred luminescence [7], and can be used as flexible inorganic spacer units for the assembly of novel heteronuclear complexes [8].

As implied by the redox-switched processes described above, it is well known that binding at a proximate site can affect the oxidation potential of the ferrocene unit [1–6]. In general, metal centres increase the redox potential by withdrawing electron density away from the ferrocene centre, whereas p-block anions and those neutral hydrogen bonding species reported so far, decrease the potential. This aspect has attracted interest from researchers interested in developing redox-active sensors for a variety of species [9]; i.e. attaching a ferrocene group to a ligand enables the binding event to be read-out using electrochemical methods. Binding at a proximate site can also affect the UV–vis properties of the ferrocene unit [3a,10]; in general, metal complexation or protonation induces bathochromic shifts in the lowest energy spin-allowed ferrocene band, which absorbs between 400 and 500 nm.

Perhaps the most studied ferrocene-containing ligands have been those containing N-donor atoms, in particular pyridine and its derivatives [1a,1b]. As would be expected, the usual species bound by ferrocene-containing pyridyl ligands are the transition metals, although s-block cations have been bound by such derivatives in the presence of other hard donor atoms [11] and neutral organic molecules have been bound

* Corresponding author. Fax: +44-1392-263-434.
E-mail address: j.h.r.tucker@exeter.ac.uk (J.H.R. Tucker).

0022-328X/01/$ - see front matter
PII: S0022-328X(01)00924-X

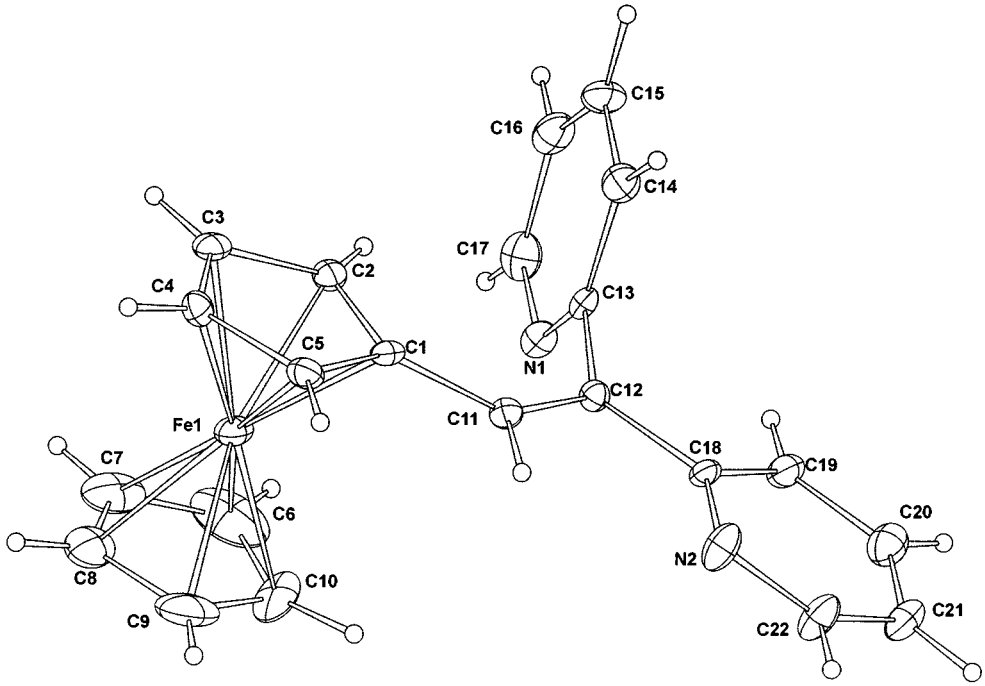

Fig. 1. X-ray structure of **1**.

through hydrogen bonds in the presence of other H-bond donor groups [6].

Here we report the effect of transition metal complexation on the electrochemical and spectroscopic properties of three ferrocene-containing pyridine ligands **1**, **2** and **3**, and examine the role of the spacer group as well as that of the ligand and complex geometry in controlling these properties.

2. Results and discussion

Compounds **1** [1b], **2** [1b] and **3** [3a] were prepared as described previously.

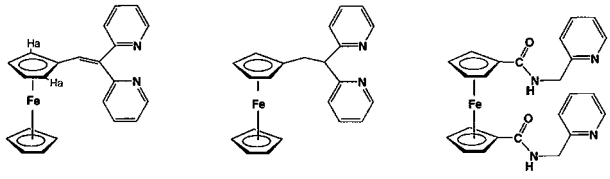

1 **2** **3**

Suitable crystals of **1** for X-ray diffraction were grown by slow diffusion of diethyl ether into a dichloromethane solution of the ligand at 275 K. The structure is presented in Fig. 1 and selected bond lengths and angles are presented in Table 1. It is interesting to note that the N2 pyridine ring is coplanar with the spacer group to maximise conjugation with the double bond (C11–C12–C18–N2 angle = 10°) whilst the two pyridyl groups are situated almost perpendicular to one another (C11–C12–C13–N1 angle = 92°), presumably to minimise steric and electronic repulsions. The Cp rings are virtually eclipsed (rotation angle = 7°).

2.1. Complex formation with Mo(0)

The complex [**1**:$Mo(CO)_4$] was synthesised by reacting **1** with [$Mo(NHC_5H_{10})_2(CO)_4$] in benzene for 24 h. As expected, ^{1}H-NMR spectrosocopy in $CDCl_3$ revealed that the two resonances corresponding to the pyridine protons adjacent to two nitrogen atoms in the free ligand (8.83 and 8.61 ppm) shift downfield upon complexation to 9.09 and 9.02 ppm, respectively. It is interesting to note that the singlet corresponding to the olefinic proton shifts upfield by 0.77 to 6.98 ppm. However, the most significant change, as found previously with the analogous Pt(II) complex [1b], is that the two signals corresponding to the two pairs of protons

Table 1
Selected bond lengths (Å) and bond angles (°) for **1**

Bond lengths			
N(1)–C(13)	1.327(6)	C(11)–C(12)	1.338(7)
N(1)–C(17)	1.341(6)	C(12)–C(13)	1.483(7)
N(2)–C(18)	1.338(6)	N(2)–C(22)	1.329(6)
C(1)–C(11)	1.475(7)	C(12)–C(18)	1.488(7)
Bond angles			
N(2)–C(18)–C(12)	117.7(4)	C(11)–C(12)–C(13)	121.2(5)
C(12)–C(11)–C(1)	128.7(5)	C(11)–C(12)–C(18)	121.1(4)
N(1)–C(13)–C(12)	117.6(4)	C(13)–C(12)–C(18)	117.6(4)

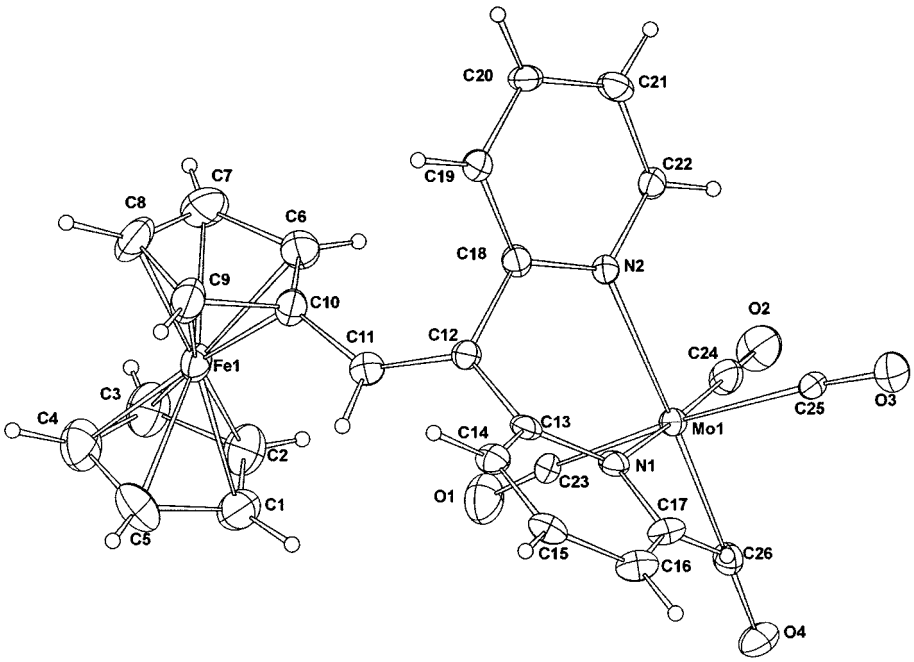

Fig. 2. X-ray structure of [**1**:$Mo(CO)_4$].

on the derivatised Cp ring of **1** split into four separate signels upon complexation.

The explanation for this change in the NMR spectra can be found from an inspection of the X-ray structure of [**1**:$Mo(CO)_4$], presented in Fig. 2. The formation of the six-membered chelate ring forces the two pyridyl units to be non-coplanar, resulting in a puckered conformation. Cremer–Pople analysis [12] shows the conformation to be boat (θ and ϕ angles = 99.3 and 178.64°, respectively). Assuming that such a geometry is retained in solution, the two proton pairs on the derivatised ring would not be equivalent, even if rotation about the C10–C11 bond were fast on the NMR time-scale. Unlike in the free ligand, neither pyridine is coplanar with the spacer group but like in the free ligand, the Cp rings are virtually eclipsed (rotation angle = 2°). Selected bond distances and angles are displayed in Table 2.

The angle between the two bonds linking the pyridine units hardly changes upon complexation. Clearly the ligand is flexible enough to coordinate to the Mo centre by appropriate rotation about the C12–C18 and C12–C13 bonds in a manner which does not change the geometry of the ferrocene and spacer units or deform the octahedral geometry about the metal centre. The equatorial M–C bonds *trans* to the Mo–N bonds are significantly shorter than the two axial Mo–C bonds, reflecting the fact that the two Mo–N bonds result in more Mo electron density being available for back-bonding to the two equatorial carbonyls. Consequently, these two ligands have longer C–O bonds. A similar effect has been observed with related Mo(0) tetracarbonyl complexes [13]. Interestingly, no reaction occurred when the reduced ligand 2 was treated with [$Mo(NHC_5H_{10})_2(CO)_4$] under a variety of conditions, which shows that the introduction of a saturated linkage between the ferrocene and the binding site must disfavour chelate ring formation, although the reasons for this are not clear.

2.2. Complex formation with Cu(I) and Zn(II)

In order to test the ability of ligands **1**, **2** and **3** to act as simple chromogenic and redox-active sensors for metal ions, metal complexes were synthesised in situ by the simple addition of an acetonitrile solution of the metal salt to the appropriate compound, predissolved in acetonitrile. The triflate salts of the alkali metals and Zn(II) were used as they have good solubility in this solvent, as does the tetrakis(acetonitrile)copper(I) salt.

Table 2
Selected bond lengths (Å) and bond angles (°) for [**1**:$Mo(CO)_4$]

Bond lengths			
N(1)–C(13)	1.355(15)	O(2)–C(24)	1.168(16)
N(1)–C(17)	1.353(16)	O(4)–C(26)	1.152(15)
N(2)–C(18)	1.374(14)	O(1)–C(23)	1.125(16)
C(10)–C(11)	1.455(18)	O(3)–C(25)	1.122(15)
C(11)–C(12)	1.338(17)		
Bond angles			
N(2)–C(18)–C(12)	119.1(10)	C(11)–C(12)–C(13)	118.3(11)
C(12)–C(11)–C(10)	129.2(13)	C(11)–C(12)–C(18)	122.3(11)
N(1)–C(13)–C(12)	119.0(10)	C(13)–C(12)–C(18)	118.7(10)

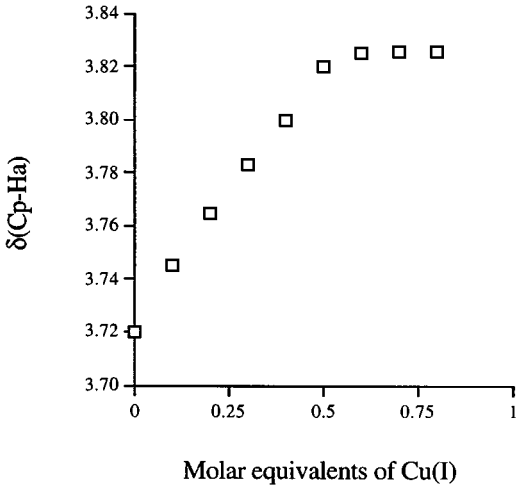

Fig. 3. ^{1}H-NMR titration of the downfield shift of the Cp–H_a resonance of **1** as a function of molar equivalents of Cu(I) in CD_3CN.

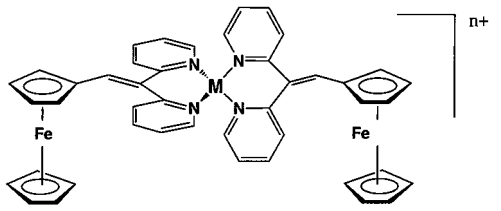

Fig. 4. Structure of the complex $[(\mathbf{1})_2\text{:Mn}]^{n+}$, M = Cu, $n = 1$ and M = Zn, $n = 2$; compound **2** forms the same dimeric complex.

Table 3
UV–vis data of compounds **1** and **3** in CH_3CN at 298 K

	λ_{max} (nm)	ε (dm^3 mol^{-1} cm^{-1})
1	464	1200
$[(\mathbf{1})_2$:Cu(I)]	496	1810
$[(\mathbf{1})_2$:Zn(II)]	486	1640
3 [a]	440	200
$[(\mathbf{3})_2$:Cu(I)]	440	250
$[(\mathbf{3})_2$:Zn(II)]	450	310

[a] Reported previously in CH_2Cl_2 in Ref. [3a].

For compounds **1** and **2**, ^{1}H-NMR studies in CD_3CN revealed shifts in the resonances corresponding to the pyridyl and Cp protons upon addition of excess Zn(II) and Cu(I), although no changes were observed upon addition of alkali metal salts. Titration experiments were carried out to evaluate the complex stoichiometry by monitoring the downfield shift of the resonances corresponding to the Cp protons upon complexation (Fig. 3). Only one set of signals was seen which indicated that exchange between free ligand and complex was fast on the NMR time-scale. Although the downfield shifts are very small, all the curves correspond to a 2/1 (ligand/metal) stoichiometry (Fig. 3), in which each metal ion can adopt a favoured pseudo-tetrahedral geometry in-between two ferrocene ligands, as depicted in Fig. 4.

A similar NMR titration experiment in CD_3CN on compound **3** did not reveal the complex stoichiometry, as upon addition of increasing amounts Zn(II) and Cu(I), precipitation occurred. However, the addition of excess metal salt as a solid to **3** in $CDCl_3$ revealed downfield shifts in the resonances corresponding to the pyridyl and Cp protons, which indicated complexation by the pyridine ligands.

Previous studies on ferrocene ligands have shown that the characteristic band between 400 and 500 nm, ascribed to the lowest energy spin-allowed d–d band of the ferrocene unit [14], is perturbed by complexation [3a,10]. Therefore, UV–vis spectroscopy was used for further complexation experiments with **3** since lower concentrations could be used. Accordingly, the addition of Zn(II) or Cu(I) to a 10^{-4} molar solution of **3** in acetonitrile resulted in an increase in absorbance in this band and in the case of Zn(II), a clear shift in the λ_{max} value to longer wavelengths (Table 3).

Titration experiments were performed on **3** where the change in absorbance at a constant wavelength was monitored upon addition of aliquots of metal salt. The titration graphs, as shown in Fig. 5 for the system with Cu(I), reveal that, as found with **1** and **2**, a 2/1 (ligand/metal) stoichiometry is favoured. This result was unexpected, since simple model studies suggested that the two amide carbonyls and two pyridine ligands could bind to the metal in a 1:1 stoichiometry. However, IR studies in acetonitrile revealed no decrease in the amide carbonyl stretching frequency of **3** (1624 cm^{-1}) upon metal complexation; in related ferrocene-containing bis-amides, this band has been shown to shift to a lower frequency when the amide carbonyls act as ligands [15]. Taking all this data into account, a schematic representation of the likely solution structure of the zinc or copper complex with **3** is depicted in Scheme 1.

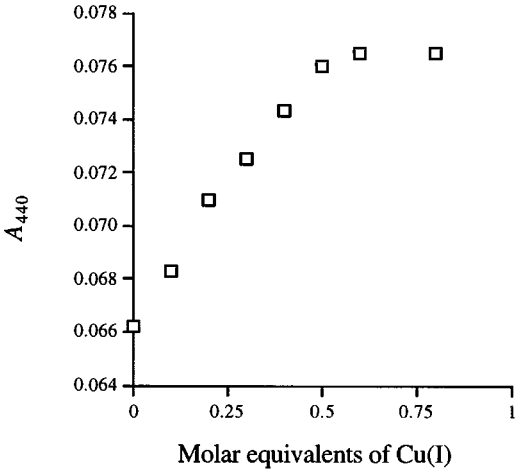

Fig. 5. UV–vis titration of the change in absorption intensity at 440 nm of **3** as a function of molar equivalents of Cu(I) in CH_3CN.

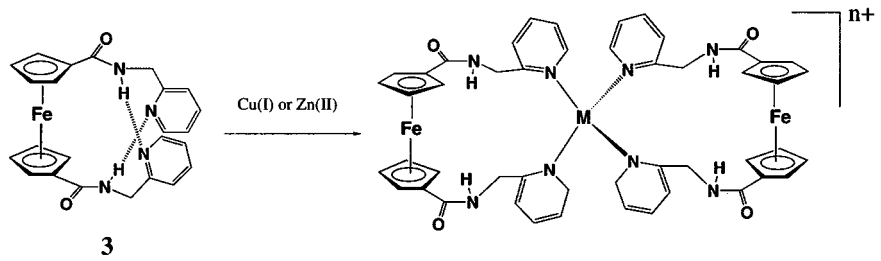

Scheme 1.

As reported previously for the protonation studies with **3** [3a], complex formation with this ligand must necessitate cleavage of the two intramolecular hydrogen bonds, as shown in Scheme 1. Accordingly, NMR studies in $CDCl_3$ revealed a large upfield shift of ca. 1.4 ppm in the resonance corresponding to the two amide protons of **3** upon addition of metal salts.

The addition of Zn(II) and Cu(I) to acetonitrile solutions of **1** resulted in similar changes to the 400–500 nm range of the UV–vis spectrum, with a bathochromic shift in the d–d band observed, accompanied by an increase in absorbance (Table 3). Titration experiments with **1** confirmed the complex stoichiometries found from the ^{1}H-NMR studies. Unfortunately, the d–d band for **2** in acetonitrile was very weak and was masked by higher energy bands, which prevented titration experiments from being performed with this ligand.

2.3. Electrochemical studies

Cyclic voltammetry experiments were carried out to assess the effect of metal complexation on the reversible Fe(II)/Fe(III) redox couple of the ligands **1**, **2** and **3**. The studies were carried out in CH_3CN solution (ca. 10^{-4} M), except for the Mo(0) complex, which was studied in CH_2Cl_2 for solubility reasons. The electrode potentials (E) for the ligands versus Ag | AgCl and shifts in electrode potential upon complexation (ΔE) are displayed in Table 4. It is clear from this data that, as expected, metal complexation perturbs the electronic properties of each ferrocene unit, making the complexes harder to oxidise than the respective free ligands.

As found previously with the Pt(II) complexes of **1** and **2** [1b], there is a much larger change in the redox potential of **1** upon Zn(II) or Cu(I) complexation than there is with **2**, due to the presence in **1** of π-electron conjugation between the binding site and the ferrocene unit. However the shifts in potential brought about by the addition of 0.5 molar equivalents of Zn(II) and Cu(I) to ligand **3**, which, like ligand **2**, has no conjugated link between the binding site and the ferrocene centre, are larger than expected. This result is all the more surprising since the addition of two molar equivalents of H^+ to **3** in CH_2Cl_2, which protonates both pyridine groups, results in a much smaller shift in potential (+15 mV) [3a]. Therefore, simple through-space electrostatic effects can not be invoked to explain these large changes in potential, since protons have a much higher charge density. Furthermore, Cu(I), which has a lower charge density than Zn(II), produces the greatest effect. It is also evident that whereas metal complexation imparts changes in the 400–500 nm region of the visible spectrum of **3** (Table 3), protonation has no effect on the λ_{max} value [3a] and the observed increase in intensity is thought to arise from bathochromic shifts in higher energy bands. In fact, previous studies have shown that there is often a correlation between the oxidation potential and the energy and intensity of the d–d band in the 400–500 nm region, as both processes involve the participation of electrons located in the Fe centred HOMO [3a,16].

The reason for this difference in the redox behaviour of **3** towards metal complexation and protonation is likely to be associated with the conformation of each complex. So that **3** can bind the metal in a 2/1 stoichiometry, the two arms of each ligand must orientate themselves close to one another in a way that maximises bond strength but minimises steric hinderance (Scheme 1). The size of the cation may also affect this conformation. Such a process would not occur upon double protonation of **3**, since charge repulsion would

Table 4
Electrochemical data for compounds **1**–**3** and their complexes in dry CH_3CN at 293 K

Compound	E/V	ΔE (mV)		
		Mo(0) complex	+Cu(I)	+Zn(II)
1	0.48 [a,b]	+190 [d]	+150	+120
2	0.41 [b]	–	+30	+70
3	0.37 [c]	–	+170	+100

[a] 0.49 V in CH_2Cl_2 at 293 K.
[b] Value reported previously in Ref. [1b] vs. decamethylferrocene as an internal reference in CH_2Cl_2.
[c] Value reported previously in Ref. [3a] vs. ferrocene as an internal reference in CH_2Cl_2.
[d] Shift in CH_2Cl_2.

place the two arms far apart. Conformational effects, such as Cp ring tilt [17], and Cp ring rotation [10b] are thought to influence the spectroscopic and redox properties of ferrocenes and it seems likely that similar processes may play a role here.

3. Conclusion

Ferrocene ligands **1**, **2** and **3** bind a range of d block metals and complexation affects the redox and chromogenic properties of the ferrocene unit in a variety of ways. The differences in redox properties between **1** and **2**, which are very similar structurally, can be readily explained using simple bond conjugation arguments. However, it appears that conformational effects have to be considered in order to explain the redox and chromogenic properties of **3** upon metal complexation. Clearly the versatile nature of the geometry of the Cp rings in ferrocene, in terms of their respective rotation and tilt, continues to offer chemists opportunities to design novel complexes with interesting spectroscopic and electrochemical properties.

4. Experimental

4.1. General comments

^{1}H- and ^{13}C-NMR spectra were recorded on a Bruker Advance DRX 400 spectrometer at 298 K. IR spectra were taken on a Nicolet magna 550 spectrometer. UV–vis spectra were recorded at 293 K on a Unicam UV4 spectrometer. EI mass spectra were carried out at the University of Wales, Swansea, UK by the EPSRC National Mass Spectrometry Service. Titration experiments were carried out by adding aliquots of a solution of the appropriate metal salt (zinc trifluoromethanesulfonate or tetrakis(acetonitrile)copper(I) hexafluorophosphate) to a solution of the ferrocene ligand (ca. 10^{-3}–10^{-4} M) in CD_3CN (for NMR studies) or CH_3CN (for UV–vis studies). The absorbance readings from the UV–vis spectra were adjusted to take into account the dilution of the solution during the course of each experiment.

4.2. Preparation of {[2,2-(di-2-pyridyl)ethenyl]-ferrocenyl}tetracarbonyl molybdenum(0), [1:Mo(CO)$_4$]

Compound **1** [1b] (0.050 g, 0.14 mmol) and $[Mo(CO)_4(NHC_5H_{10})_2]$[18] (0.053 g, 0.14 mmol) in anhydrous benzene (30 ml) were refluxed for 24 h under an atmosphere of N_2. Pure compound precipitated out overnight and was collected by filtration, then washed with anhydrous benzene (3 × 5 ml) to give a red solid (0.052 g, 64%). The compound was recrystallised from CH_2Cl_2–diethyl ether to give red crystals suitable for X-ray analysis, m.p. 240 °C (decomp.); ^{1}H-NMR ($CDCl_3$) 9.09 (d, 1H, py–H), 9.02 (d, 1H, py–H), 7.80 (t, 1H, py–H), 7.58 (t, 1H, py–H), 7.52 (t, 1H, py–H), 7.20 (d, 1H, py–H), 7.16 (d, 1H, py–H), 7.10 (d, 1H, py–H), 6.98 (s, 1H, olefin–H), 4.43 (m, 1H, Cp–H), 4.37 (m, 1H, Cp–H), 4.18 (m, 1H, Cp–H), 4.17 (s, 5H, Cp–H), 3.65 (m, 1H, Cp–H); ν_{max}/cm^{-1} (CH_2Cl_2); 2003, 1915, 1891; m/z (EI) 576 [M^+], accurate mass Calc. for $C_{26}H_{18}FeMoN_2O_4$: 575.9671. Found: 575.9676.

Table 5
Crystal data and structure refinement for compounds **1** and [**1**:Mo(CO)$_4$]

	1	[**1**:Mo(CO)$_4$] **2**
Empirical formula	$C_{22}H_{18}N_2Fe$	$C_{26}H_{18}N_2O_4FeMo$
Formula weight	366.23	574.22
Crystal system	Orthorhombic	Triclinic
Space group	$P2_12_12_1$	$P\bar{1}$
a (Å)	7.5921(11)	8.144(2)
b (Å)	14.9902(9)	9.226(2)
c (Å)	15.372(2)	18.790(4)
α (°)	90.0	79.22(3)
β (°)	90.0	85.63(3)
γ (°)	90.0	66.77(3)
V (Å^3)	1749.4(4)	1274.5(5)
Z	4	2
D_{calc} (Mg m^{-3})	1.390	1.653
Absorption coefficient (mm^{-1})	0.867	1.103
$F(000)$	760	636
Crystal size (mm^3)	0.28 × 0.16 × 0.12	0.55 × 0.03 × 0.02
θ_{max} (°)	25.04	26.37
Observed reflections collected	7635	20492
Independent reflections	2717	5143
R_{int}	0.0884	0.0805
Final R indices ($I>2\sigma I$)	$R_1 = 0.0422$, $wR_2 = 0.0937$	$R_1 = 0.0542$, $wR_2 = 0.1392$
Final R indices (all data)	$R_1 = 0.0541$, $wR_2 = 0.0962$	$R_1 = 0.0833$, $wR_2 = 0.1551$
ρ max/min (e Å^{-3})	0.568/−0.315	0.761 and −0.706

4.3. X-ray crystallography

Crystals of compounds **1** and [**1**:Mo(CO)$_4$] were mounted on glass fibres using the oil drop technique and intensity data collected at 150(2) K. A summary of crystal data, data collection strategy and model refinement parameters is given in Table 5. Data were measured on a FAST TV area detector diffractometer with a rotating anode target ($\lambda_{Mo-K_\alpha} = 0.71069$ Å), following previously described procedures [19]. The structures were solved via direct methods (SHELXS-86) [20], and then subjected to full matrix least-squares refinement on F_o^2 (SHELXL-93) [21]. For all structures non-hydrogen

atoms were made anisotropic, with hydrogens in calculated positions (C–H = 0.96 Å, with U_{iso} tied to U_{eq} of the parent atoms). Data were corrected for absorption effects using the semi empirical method of DIFABS [22].

4.4. Electrochemistry

Cyclic voltammograms were recorded at 293 K in dry CH_2Cl_2 or dry CH_3CN using an EG&G 273 potentiostat or a BAS 100B/W electrochemical workstation. Electrode potentials, E, where $E = 0.5\ (E_{pa} + E_{pc})$ were referenced to a Ag | AgCl reference electrode. The confidence limit is ± 10 mV. Pt working and Pt counter electrodes were used with tetrabutylammonium perchlorate (0.1 M) as supporting electrolyte, scan rate = 100 mV s^{-1}. For each voltammogram, the reversibility of the redox wave matched that of ferrocene under the same experimental conditions ($\Delta E_p^\circ = 70$–100 mV).

5. Supplementary material

Crystallographic data for the structural analysis have been deposited with the Cambridge Crystallographic Data Centre, CCDC Nos. 154890 and 154891. Copies of this information may be obtained free of charge from The Director, CCDC, 12 Union Road, Cambridge CB2 1EZ, UK (fax: +44-1233-336-033; e-mail: deposit@ccdc.cam.ac.uk or www: http://www.ccdc.cam.ac.uk).

Acknowledgements

We thank the University of Exeter for the award of a University Research Studentship (to J.D.C).

References

[1] (a) P. Zanello, in: A. Togni, T. Hayashi (Eds.), Ferrocenes: Homogeneous Catalysis, Organic Synthesis, Materials Science, Ch. 7, VCH, Weinheim, 1995;
(b) J.D. Carr, S.J. Coles, M.B. Hursthouse, M.E. Light, E.L. Munro, J.H.R. Tucker, J. Westwood, Organometallics 19 (2000) 3312 and references therein;
(c) H. Plenio H, C. Aberle, Chem. Commun. (1998) 2697 and references therein.

[2] (a) P.D. Beer, Chem. Soc. Rev. 18 (1989) 409;
(b) J.L. Medina, T.T. Goodnow, M.T. Rojas, J.L. Atwood, B.L. Lynn, A.E. Kaifer, G.W. Gokel, J. Am. Chem Soc. 114 (1992) 10583;
(c) T. Saji, I. Kinoshita, J. Chem. Soc. Chem. Commun. (1986) 716.

[3] (a) J.D. Carr, S.J. Coles, W.W. Hassan, M.B. Hursthouse, K.M.A. Malik, J.H.R. Tucker, J. Chem. Soc. Dalton Trans. (1999) 57 and references therein;
(b) H. Plenio, J. Yang, R. Diodone, J. Heinze, Inorg. Chem. 33 (1994) 4098.

[4] P.D. Beer, J. Cadman, J.M. Lloris, R. Martínez-Mánez, J. Soto, T. Pardo, M.D. Marcos, J. Chem. Soc. Dalton Trans. (2000) 1805 and references therein.

[5] P.D. Beer, E.L. Tite, A. Ibbotson, J. Chem. Soc. Dalton Trans. (1991) 1691.

[6] (a) J.D. Carr, S.J. Coles, M.B. Hursthouse, M.E. Light, J.H.R. Tucker, J. Westwood, Angew. Chem. Int. Ed. Engl. 39 (2000) 3296 and references therein;
(b) J.D. Carr, L. Lambert, D.E. Hibbs, M.B. Hursthouse, K.M.A. Malik, J.H.R. Tucker, Chem. Commun. (1997) 1649 and references therein.

[7] A.C. Benniston, V. Goulle, A. Harriman, J.M. Lehn, J. Phys. Chem. 98 (1994) 7798.

[8] M. Buda, J.C. Moutet, E. Saint-Aman, A. De Cian, J. Fischer, R. Ziessel, Inorg. Chem. 37 (1998) 4146.

[9] L.M. Goldenberg, M.R. Bryce, M.C. Petty, J. Mater. Chem. 9 (1999) 1957.

[10] (a) P.D. Beer, D.K. Smith, J. Chem. Soc. Dalton Trans. (1998) 417;
(b) C.D. Hall, I.P. Danks, N.W. Sharpe, J. Organomet. Chem. 390 (1990) 227;
(c) A. Chesney, M.R. Bryce, A.S. Batsanov, J.A.K. Howard, L.M. Goldenberg, Chem. Commun. (1998) 677;
(d) R.J. Less, J.L.M. Wicks, N.P. Chatterton, M.J. Dewey, N.L. Cromhout, M.A. Halcrow, J.E. Davies, J. Chem. Soc. Dalton Trans. (1996) 4055.

[11] C.D. Hall, J.H.R. Tucker, S.Y.F. Chu, A.W. Parkins, S.C. Nyburg, Chem. Commun. (1993) 1505.

[12] D. Cremer, J.A. Pople, J. Am. Chem. Soc. 97 (1975) 1354.

[13] R.J. Blau, U. Siriwardane, Organometallics 10 (1991) 1627.

[14] Y.S. Sohn, D.N. Hendrickson, H.B. Gray, J. Am. Chem Soc. 93 (1971) 3603.

[15] C.D. Hall, I.P. Danks, M.C. Lubienski, N.W. Sharpe, J. Organomet. Chem 384 (1990) 139.

[16] (a) J.C. Calabrese, L.T. Cheng, J.C. Green, S.R. Marder, W. Tam, J. Am. Chem Soc. 113 (1991) 7227;
(b) M.M. Bhadhade, A. Das, J.C. Jeffery, J.A. McCleverty, J.A. Navas Badiola, M.D. Ward, J. Chem. Soc. Dalton Trans. (1995) 2769;
(c) M.E.N.P.R.A. Silva, A.J.L. Pombeiro, J.J.R. Frausto da Silva, R. Herrmann, N. Deus, R.E. Bozak, J. Organomet. Chem. 480 (1994) 81 and references therein.

[17] T.H. Barr, W.E. Watts, Tetrahedron 24 (1968) 6111.

[18] D.J. Darensbourg, R.L. Kump, Inorg. Chem. 17 (1978) 2680.

[19] S.R. Drake, M.B. Hursthouse, K.M.A. Malik, S.A.S. Miller, Inorg. Chem. 32 (1993) 4653.

[20] G.M. Sheldrick, Acta Crystallogr. Sect. A 46 (1990) 467.

[21] G.M. Sheldrick, University of Göttingen, Göttingen, Germany, 1993 (unpublished work).

[22] N.P.C. Walker, D. Stuart, Acta Crystallogr. Sect. A 39 (1983) 158 adapted for FAST geometry by A. Karaulov, University of Wales, Cardiff, 1991.